

FIELD ERRORS IN THE BOOSTER BENDING MAGNETSAND QUADRUPOLES AND POSSIBLE COMPENSATION METHODS

M. Giesch

Summary

Besides statistical errors given by the variation of magnetic characteristics of the steel supply and mechanical tolerances of the iron cores and coils, systematic errors are caused within individual units by the special geometry of the Booster bending magnets and quadrupoles. An estimate of these errors for different types of steel has already been given previously <sup>(1)</sup>. In the meantime a choice of the steel for the prototype bending magnet and quadrupole was made and a more detailed study of different errors and compensation methods has been done, which are summarized in this report.

## 1. INTRODUCTION

Tight tolerances are imposed on the field variation of the Booster bending magnets and quadrupoles. The relative field error over the useful aperture in all bending magnets and quadrupoles is given to

$$\langle \Delta B/B \rangle \text{ rms} \leq 5 \cdot 10^{-4} \text{ for the bending magnets}$$

and

$$\langle \Delta g/g \rangle \text{ rms} \leq 2 \cdot 10^{-3} \text{ for the quadrupoles.}$$

A careful selection of commercially available steel, with low coercivity, high permeability for the induction range, small variation of these parameters and adequate specifications of mechanical tolerances for the core fabrication are necessary, in order to obtain the required field precision. When this cannot be met by these requirements alone, simple compensation methods have to be employed.

Alignment errors for magnets and quadrupoles, which can normally be treated separately, have also to be taken into account for the core design and may cause additional errors. This is due to the special Booster geometry, which does not allow an individual alignment of the four vertically combined bending magnet and quadrupole units.

A cross sectional view of the bending magnets and quadrupoles is shown in fig. 1 and fig. 2. The iron cores are laminated and made from 1 mm thick electro-graded silicon steel sheet with magnetic characteristics as given in fig. 3. Since silicon steel has always some orientation the values refer to measurements on CERN standard

ring samples, in which the individual rings are piled such that their relative orientation in respect to the rolling direction is maintained. The magnets and quadrupoles are series connected. A pulsed excitation current is used, having a rise time of 0.6 s and a flat top of 0.08 sec.

In the following, it is distinguished between statistical errors which are related to the entire magnet system and systematic errors related to individual units. Only the specified steel characteristics are used for the calculations.

## 2. STATISTICAL ERRORS

Statistical errors affect the integral field from block to block, giving a variation of bending power for the 33 bending magnet units and of gradient power for the 17/33 quadrupole units. They are caused by the mechanical tolerances of the core dimensions and by the spread of the magnetic characteristics of the steel supply.

### 2.1 Mechanical tolerances of the iron cores and coils

The tolerances of core length and aperture specified for the prototype bending magnet and quadrupole are listed in Tables 1 and 2, together with the resulting integral field errors. Errors, due to a variation of the coil length, are small for the specified tolerances and can be neglected. The positioning of the coil within the aperture is however rather critical (see para. 3).

Tolerances related to the relative position of the four apertures within one unit are only critical for the quadrupoles. The tolerance for spacing of quadrupole centres was specified to  $\pm 0.04$  mm. The resulting error on the closed orbit is given in ref. 2.

## 2.2 Variation of magnetic characteristics of the steel supply

For the production of large quantities of steel sheets a certain allowance has to be made regarding the spread of permeability and coercivity of the total steel supply. In general, a variation of  $\pm 10\%$  for the permeability and coercivity can be expected.

### 2.2.1 Variation of permeability

$$\text{From } B = \frac{\mu_0 NI}{cli/\mu + la}$$

one gets for the relative error in bending power

$$\Delta B/B = \frac{\Delta\mu}{\mu^2} \frac{cli}{la} \quad (1)$$

with  $cli/la \approx 10$ , we have for bending magnets

$$\Delta B/B (\text{‰}) = \pm \frac{\Delta\mu}{\mu} (\text{‰}) \times \frac{100}{\mu} \quad (2)$$

and with  $cli/la \approx 5.5$  (40 mm from the centre of the quadrupoles), the error in gradient power is

$$\Delta g/g (\text{‰}) = \pm \frac{\Delta\mu}{\mu} (\text{‰}) \times \frac{55}{\mu} \quad (3)$$

### 2.2.2 Variation of coercive force

The variation of remanent field between blocks due to the variation of the coercive force throughout the steel supply is given by :

$$\Delta B = \mu_0 \Delta H_c c l_i / l_a \quad (4)$$

with  $B_{inj} = 0.126 \text{ T}$  and  $B_{tr} = 0.59 \text{ T}$ ,

the relative error for the bending magnets is :

$$\begin{aligned} \Delta B / B_{inj} \text{ (}^\circ\text{/}^\circ\text{)} &= \pm 10 \Delta H_c \text{ (A/cm)} \\ \Delta B / B_{tr} \text{ (}^\circ\text{/}^\circ\text{)} &= \pm 2.1 \Delta H_c \text{ (A/cm)} \end{aligned} \quad (5)$$

For the quadrupoles we have with  $\Delta B / B \propto \Delta g / g$   
( $B = 320/1500 \text{ G}$  for  $Z = 0$ ,  $X = 40 \text{ mm}$ ).

$$\begin{aligned} \Delta g / g_{inj} \text{ (}^\circ\text{/}^\circ\text{)} &= \pm 21 \Delta H_c \text{ (A/cm)} \\ \Delta g / g_{tr} \text{ (}^\circ\text{/}^\circ\text{)} &= \pm 4,3 \Delta H_c \text{ (A/cm)} \end{aligned} \quad (6)$$

The statistical errors calculated with the formulae given above are listed in Table 1 for the bending magnets and in Table 2 for the quadrupoles. The calculations are based on the specified steel characteristics.

The permeability is defined by the magnetization curve  $B = f(H)$  of the steel (normal magnetization curve). By using these values in formulae (2) and (3) a correct result, within the precision of this calculation, is only obtained for transfer fields.

For injection fields the working point(s) in the iron is found in the second quadrant of the hysteresis loop, as schematically indicated in fig. 4. No proper  $\mu$ -values can be defined in this region. Because of the smaller slope of the upgoing branch of the hysteresis curve, too optimistic results would be obtained by using the permeability values given by the magnetization curve. To account for this, the  $\mu$ -values given in fig. 3 were reduced by 20 % for the calculation of the error at injection.

### 3. SYSTEMATIC ERRORS OF BENDING MAGNETS AND QUADRUPOLES

#### 3.1 Bending magnets

Systematic deviations from the ideal field distribution within the aperture of bending magnets are given mainly by the geometry of the iron core and the excitation coils. In addition one has for the Booster magnets systematic field differences between the four gaps of one magnet unit. We see from fig. 1 that the reluctance is different for the two outer magnets (gaps 1 and 4). This gives a corresponding field difference, since all gaps have the same excitation current.

The field in the air gap of the outer magnets is :

$$B_1 = \mu_0 NI/la - \mu_0 \sum H_i l_i / la \quad (7)$$

For the field of the inner magnets, we have correspondingly

$$B_2 = \mu_0 NI/\ell a - \mu_0 \sum H_2 \ell_2 / \ell a \quad (8)$$

The second term in these equations represents the slope of the air gap lines schematically indicated in fig. 4.

The field error between inner and outer magnets is thus

$$\Delta B = B_1 - B_2 = \mu_0 (\sum H_2 \ell_2 - \sum H_1 \ell_1) / \ell a \quad (9)$$

Because  $\ell_1 > \ell_2$

$H > 0$  for transfer field

$H < 0$  for injection field

the field in the outer magnets will be smaller at transfer and higher at injection field level compared to the field in the inner gaps.

A computer programme has recently been developed by C. Iselin<sup>(3)</sup>, being able to cope with multi-gap magnets. Computer calculations could thus be done for the Booster bending magnets for transfer field level<sup>(4)</sup>. The results are given in fig. 5, where the field distribution within the aperture of inner and outer magnets is shown. The curves summarize all systematic errors for transfer field level, for an ideal pole profile and a symmetrical positioning of the excitation coils. The integral field will depend on the fringe field distribution and is not known precisely at this stage.

The calculations were done with permeability values corresponding to the specified steel, assuming an isotropic distribution of magnetic characteristics in the lamination. The relative field difference between inner and outer magnets around the centre of the gap is  $\Delta B/B_{tr} = 0.8 \text{ } ^\circ/\text{oo}$ . The difference of the gradient is very small, it is almost zero for the inner gaps and about 0.06 G/cm for the outer gaps, referred to parallel poles.

Due to manufacturing tolerances a precise positioning of the coil within the aperture will not be possible. Fig. 6 shows the field distribution of the inner gaps given by a displacement of the coil by  $\Delta Z = + 0.3 \text{ mm}$ . While the field around the centre of the aperture is practically unchanged, considerable differences are given near the coils, compared to a symmetrical coil.

Since the orientation of the steel could not be taken into account by the computer programme, the results given above are somewhat optimistic. The flux lines in the outer magnets are partly running at a right angle to the rolling direction of the laminations and bigger field differences between inner and outer magnets can be expected. An estimate of the error, taking the orientation of the steel into account has been obtained in the following way :

The direction of the flux lines in the iron is known from flux plots for transfer and injection field level, obtained from computer calculations. They are valid for a wide range of magnetization curves and may safely be used. With the magnetization curves measured for different angles against the rolling direction of the steel sheet (fig. 7) we obtain from equation (9) for transfer :

$$\Delta B/B_{tr} = \mu_0 (H_2 // \ell_2 // - \sum_{\varphi=0}^{90^\circ} H_1 \varphi \ell_1 \varphi) / B_{tr} \ell a = - 1.0 \text{ } ^\circ/\text{oo} \quad (10)$$



For calculating the error at injection field level, the hysteresis loop of the iron has to be considered. Computer calculations can therefore not be done with existing programmes. One can see from fig. 4 that

$$- H_1 \approx - H_2 \approx H_c$$

Following the same principle as for transfer field, we obtain for the relative error at injection field level near the centre of the aperture :

$$\Delta B/B_{tr} = \mu_0 (H_{c//} \ell_{1//} + H_{c\perp} \ell_{1\perp} - H_{c//} \ell_{2//})/B_{inj} \ell a = 0.9 \text{ } ^\circ/\text{oo} \quad (11)$$

The field is higher in the outer gaps. The gradient having a negative slope for transfer field has a positive slope for injection field. Because the flux lines in the C shaped regions of the magnet are more concentrated for low fields, the absolute value of the gradient is expected to be somewhat smaller than given for transfer field.

Eddy currents induced in the 23 mm thick end plates of the iron core give rise to additional field errors, i.e. a variation of integral field between injection and transfer.

Detailed calculations have been made in ref. (5).

Little is known about the effect of the fringe field on the integral field distribution for bending magnets and quadrupoles. Measurements on a C shaped magnet were done (ref. 6) indicating the range of errors. Because of the different geometry and different steel characteristics of this magnet, a prediction of the errors in the Booster bending magnet cannot be done from these measurements. Provision is made for the prototypes in order to find experimentally the optimal end profile.

### 3.2 Quadrupoles

The variation of the gradient along the main axes of the quadrupole caused by the truncation of the pole profile and the coil geometry is given in fig. 8. The curves have been obtained from computer calculations, assuming infinite permeability in the iron (ref. 4). An estimate of the amplitude of higher harmonics in the quadrupole, for the given mechanical tolerances of aperture and pole position, was also given in ref. 4.

As for the bending magnets, systematic errors exist within the apertures of the four quadrupoles of one unit.

For the inner quadrupoles the gradient is different along the x and y axes. For the upper and lower quadrupoles a difference exists on the negative z axis and the positive z axis respectively. Computer calculations, as for the bending magnet, cannot be made for the quadrupole with existing programmes. In order to get a rough estimate of the systematic error, measurements have been made on analog models (stainless steel plates) assuming infinite permeability. The anisotropic distribution of the magnetic characteristics in the iron has been simulated by increasing the horizontal dimensions of the model by the factor  $\sqrt{\mu_H/\mu_L}$  for the case that the rolling directions of the steel coincides with the vertical axis of the quadrupole.

For the second case, i.e. rolling direction coinciding with the horizontal quadrupole axes, the vertical dimensions of the model were increased by the same factor as above.

By transforming the flux lines, obtained from the model in this way, to natural scale, the real flux distribution in the lamination is found. The result is given in fig. 9, where only one flux line is shown for each case. Even though the method is rather inaccurate, it can be clearly seen that the systematic error is considerably reduced by stamping the laminations such that the rolling direction of the steel sheet coincides with the horizontal quadrupole axes. This solution has been adopted for the prototype quadrupole.

It is difficult to predict an absolute value of the systematic error, but one may conclude that the gradient error at transfer is smaller than  $1^{\circ}/\infty$ .

#### 4. COMPENSATION OF ERRORS

The field errors in bending magnets and quadrupoles given in the preceding paragraphs are partly exceeding the tolerable limit. Some compensation, at least of the systematic errors, will be necessary.

##### 4.1 Steel mixing

Statistical errors caused by the variation of magnetic characteristics of the steel supply can be reduced by steel mixing, a technique generally employed for accelerator magnets. The remaining error is given in Table 1 for the bending magnets and in Table 2 for the quadrupoles. A reduction of the statistical magnetic error by a factor of 5 was assumed, due to a shuffling of the steel sheets.

Because of the dominating effect of the mechanical tolerances, practically nothing can be gained for the quadrupoles.

For the bending magnets, a small improvement is obtained for injection field level, but no change is found for the field at transfer.

No steel mixing has therefore been foreseen for the construction of the quadrupoles. For the bending magnets it will not be justified, if a considerable amount of extra costs is involved.

##### 4.2 Compensation of systematic errors at injection

The systematic field difference within the apertures of bending magnets and quadrupoles caused by the remanent field, can be reduced by a simple method proposed by G. Brianti <sup>(7)</sup>. Instead of running the Booster cycle between injection and transfer field level as originally foreseen, the minimum current of the Booster

cycle may be reduced to a value inferior to the injection current. In this case, the upgoing branch of the hysteresis loop (fig. 4) intersects with the air gap lines, corresponding to injection excitation, at lower H values ( $H^{\text{sc}}$  in fig. 4), which should be used instead of  $H_c$  in equations (11) and (13).

A complete compensation of errors can, however, not be expected since different points in the iron will follow different hysteresis loops, because of the spread of induction values and the orientation of the steel. A reduction by a factor 3 has been assumed for the values given in Table 3.

The remaining error of the bending magnets can, when necessary, be further reduced by a compensation current fed directly via the main excitation windings. The bending magnet units will be connected such that first all outer gaps are series connected, followed by a series connection of all inner gaps. A single correction power supply may be placed directly across the excitation windings of the outer or inner magnets <sup>(8)</sup>. For the quadrupoles, copper bars are foreseen for this purpose in each coil window, which can be series connected for all quadrupoles.

The optimization of the Booster cycle will be done experimentally on the prototypes. Different results may be obtained for bending magnet and quadrupole. Because an additional correction is easier to obtain for the bending magnets, the optimization shall be done for the quadrupole. The gradient in the bending magnets will by this method also be reduced to some extent.

#### 4.3 Corrections of errors at transfer field level

##### 4.3.1 Pulsed correcting current

For the bending magnets a pulsed current corresponding to the Booster cycle may be used for correcting the systematic field difference between gaps. A single power supply as mentioned in

para. 4.2 would be needed. If the current pulse has an adjustable negative flat top, a correction at injection field level will be possible at the same time. A correction of the systematic error to about  $0.1 \text{ }^{\circ}/\text{oo}$  may be possible (Table 3).

For the quadrupoles no correction for transfer field seems to be necessary, but correcting bars, as provided for the prototype, will also be foreseen for the series quadrupoles. If necessary, a further reduction of errors would be possible.

The effect of the systematic error on higher harmonics of the quadrupole has still to be studied.

#### 4.3.2. Shimming of bending magnets

The integral field around the centre of all magnet gaps can be made equal within the accuracy of measurements by shimming of the magnet ends. Shims of 0.1 mm thickness screwed on to the end-plates will allow a correction in steps of  $0.06 \text{ }^{\circ}/\text{oo}$ . The statistical and the systematic error at transfer will thus be reduced to about  $0.1 \text{ }^{\circ}/\text{oo}$ .

The statistical error at injection is also reduced. Since the mechanical tolerances have been corrected for the transfer field, only the difference of the magnetic errors between injection and transfer of Table 1 remains at injection field level. The remaining systematic error, after optimization of the cycle, can be corrected via the main excitation windings of the inner gaps.

The errors after shimming of all magnet gaps for transfer and correction at injection are given in Table 3. The statistical errors refer to the values "without steel mixing" of Table 1.

Shimming of the magnets has several advantages :

- The magnet gaps can be individually adjusted, the errors can therefore be reduced to a minimum.
- The correction is permanent and continuous observation during operation as in case of a correcting current is not necessary.
- The extremely tight tolerance for the gap height of the finished core can be relaxed. Manufacturing difficulties are reduced and cost can be saved.
- Steel mixing will not be necessary when the tolerances for the magnetic characteristics of the steel supply are kept by the steel manufacturer. A further decrease of cost can be expected.

A small disadvantage may be seen by the fact that the total measuring time will be increased slightly.

#### 4.4 Correction of radial field distribution for bending magnets

The radial field variation due to the coil geometry and the effect of end field can partly be compensated by radially shaped shims. For the prototype an opening has been foreseen in the endplates into which shims of dimensions 30 x 15 mm can be placed, mainly for investigating the optimal end profile of the magnets. For the series production of magnets a similar arrangement will be used.

#### 4.5 Correction of quadrupole end field

Nothing is known about the quadrupole end field and its harmonic content. As for the bending magnets the optimal end profile has to be found experimentally on the prototype. Shims which can be mounted on to the endplates have been foreseen for this purpose.

REFERENCES

- (1) A. Ašner : Field errors in Booster bending magnets  
M. Giesch and quadrupoles.  
SI/Note MAE/68-3
- (2) SI Parameter Meetings Nos. 21 and 22 Minutes  
SI/Mi DL/68-23
- (3) C. Iselin : Programme Magnet T 600
- (4) C. Iselin : Status of the field calculations for  
the Booster bending magnets and quadrupoles  
SI/Note MAE/68-12
- (5) A. Ašner : Eddy currents in pulsed magnets  
B. Brianti (Example of the Booster bending magnet)  
I. Gumowski SI/Int. DL/69-2
- (6) K.D. Lohmann : Magnetic measurements on a 1.5 m bending magnet  
for slow ejection at medium fields (1 to 5 kG)  
SI/Note MAE/69-1
- (7) G. Brianti : Private communication
- (8) M. Giesch : Notes on the meeting of 30th August, 1968  
SI/Mi. MAE/68-1

Distribution (open) :

List SI/2

PS/7118/gf



## Statistical Errors of Bending Magnets in Units of $10^{-4}$

Error	Tolerance	$\epsilon$ max		$\langle \epsilon \rangle$ rms				Observation
		inj	trans	without steel mix inj	steel mix trans.	with steel mix. inj	with steel mix. trans	
<u>1. mechanical</u>								
1.1 gap height	$\pm 0.025$ mm	$\pm 3.6$	$\pm 3.6$	1.8	1.8	1.8	1.8	diviation 2G
1.2 Length of core	$\pm 0.2$ mm	$\pm 1.3$	$\pm 1.3$	0.7	0.7	0.7	0.7	
<u>2. magnetic</u>								
2.1 $\Delta H_c$	$\pm 0.03$ A/cm	$\pm 3.0$	$\pm 0.6$	1.5	0.3	0.3	0.06	Factor 5 reduction by steel mixing
2.2 $\Delta \mu/\mu$								
2.3 $\Delta H_c$	$\pm 0.2$ A/cm	$\pm 0.7$	$\pm 0.14$	0.35	0.07	0.35	0.07	
2.4 $\Delta \mu/\mu$								
$\frac{\Delta B}{B} \times \frac{\sum l_{plates}}{l_{Block}}$								
Total rms Error $\sqrt{\sum (\langle \epsilon \rangle_{rms})^2} \times 10^4$				3.1	2.1	2.0	1.9	

Laminations

$$\mu_{inj} = 2600 \text{ (reduced value)}$$

$$\mu_{tr} = 6400$$

End plates

$$\mu_{inj} = 1000$$

$$\mu_{tr} = 2100$$

Table 1

## Statistical Errors of Quadrupoles $\Delta g/g$ [‰]

Error	Tolerance	$E_{max}$		$\langle \epsilon \rangle_{rms}$				Observation
		ing	trans	without steel mix		with steel mix.		
				ing	trans	ing	trans	
<u>1. mechanical</u>								
1.1 diameter of inscr. circle	$\pm 0.1 \text{ mm}$	$\pm 0.84$	$\pm 0.84$	0.42	0.42	0.42	0.42	deviation 2 $\sigma$
1.2 Length of core QD QF	$\pm 0.2 \text{ mm}$ $\pm 0.1 \text{ mm}$	$\pm 0.23$	$\pm 0.23$	0.12	0.12	0.12	0.12	
<u>2. magnetic</u>								
2.1 $\Delta H_c$ } Laminations	$\pm 0.03 \text{ A/cm}$	$\pm 0.6$	$\pm 0.13$	0.3	0.07	0.06	0.02	Factor 5 reduction by steel mixing
2.2 $\Delta \mu/\mu$ }	$\pm 10\%$	$\pm 0.28$	$\pm 0.11$	0.14	0.05	0.03	0.01	
2.3 $\Delta H_c$ } End plates	$\pm 0.2 \text{ A/cm}$	$\pm 0.26$	$\pm 0.05$	0.13	0.03	0.13	0.03	$\frac{\Delta g}{g} \times \frac{\sum l_{plates}}{l_{QF}}$ !
2.4 $\Delta \mu/\mu$ }	$\pm 15\%$	$\pm 0.1$	$\pm 0.04$	0.05	0.02	0.05	0.02	
Total rms Error $\sqrt{\sum (\langle \epsilon \rangle_{rms})^2}$ [‰]				0.57	0.45	0.46	0.44	

Laminations

$\mu_{in} = 2000$  (reduced value)

$\mu_{tr} = 5000$

End plates

$\mu_{ing} = 500$

$\mu_{tr} = 1500$

Table 2

Errors of Bending Magnets  $\Delta B/B$  [‰]

Error	Without Compensation		correcting current for inj. and transfer + optimisation of cycle		trimming of all gaps at trans. correcting current for inj.	
	inj.	trans.	inj.	trans.	inj.	trans.
Statistical	0.3	0.2	0.3	0.2	0.16	} 0.1
Systematic	0.9	1.0	0.1	0.1	0.1	

Errors of Quadrupoles  $\Delta g/g$  [‰]

Error	Without compensation		optimisation of cycle	
	inj.	trans.	inj.	trans.
Statistical	0.6	0.5	0.6	0.5
Systematic	?	< 1.0	?	< 1.0

Table 3

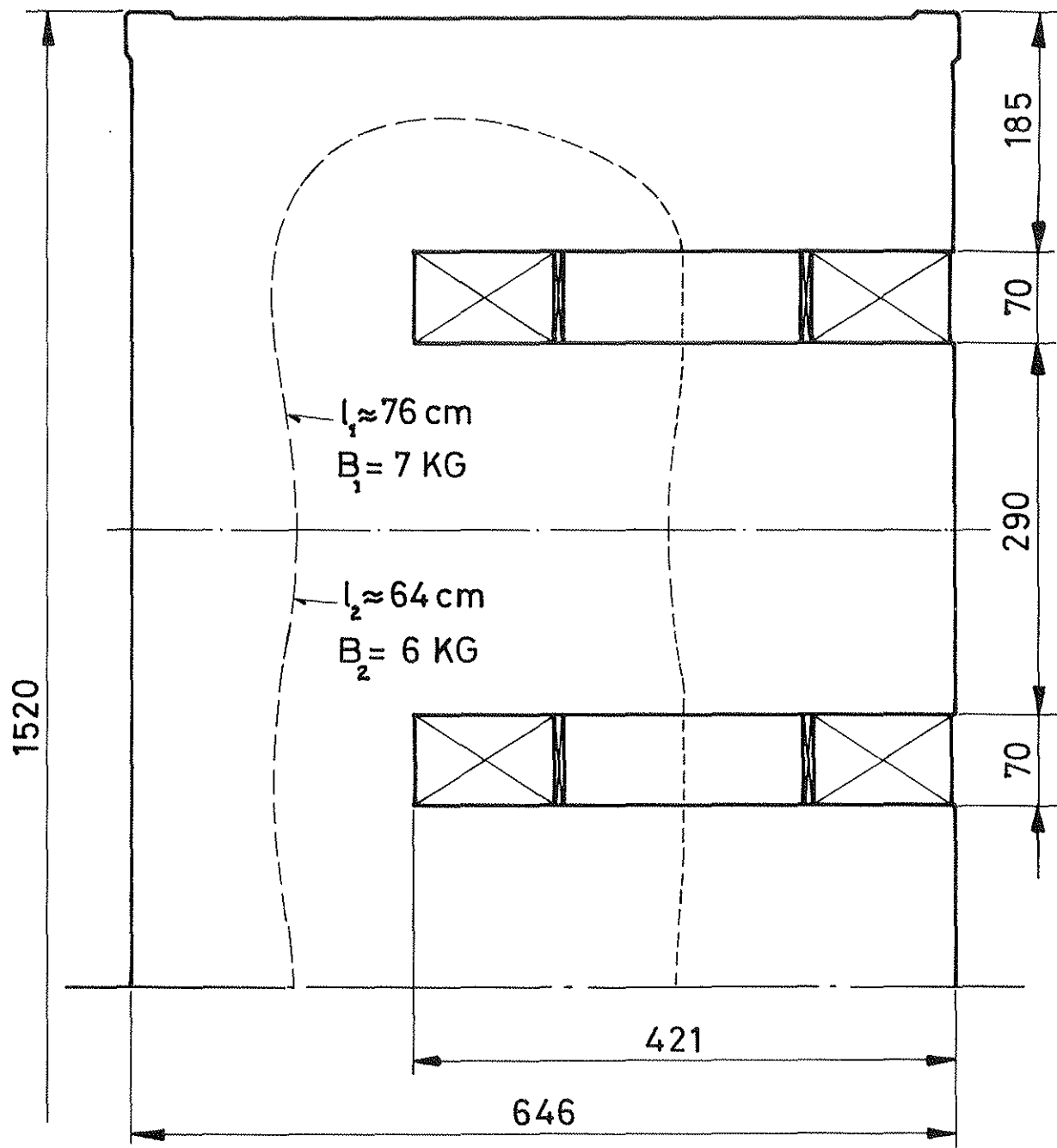


Fig1. Cross-section of Bending Magnets.

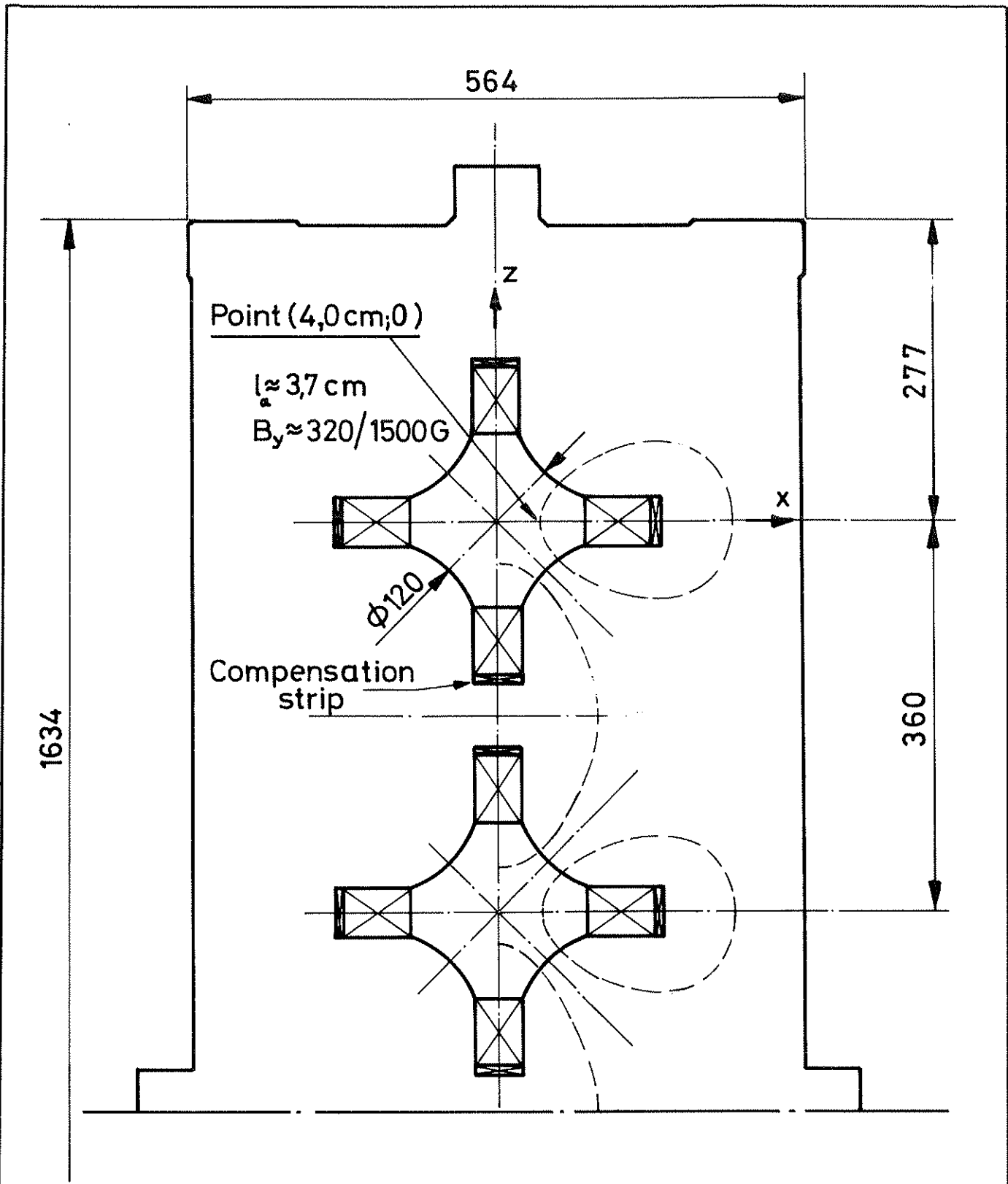


Fig 2. Cross-section of Quadrupoles

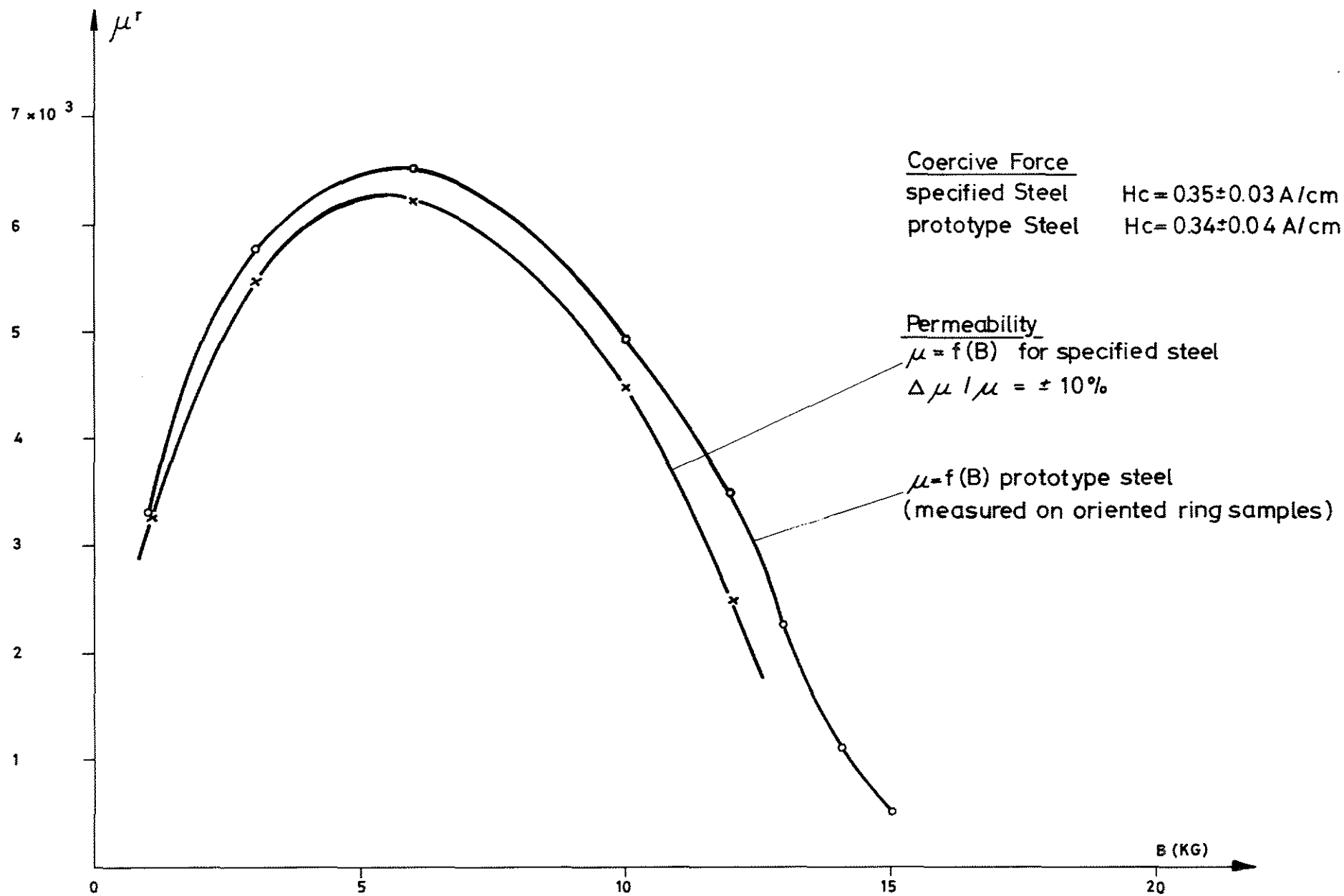
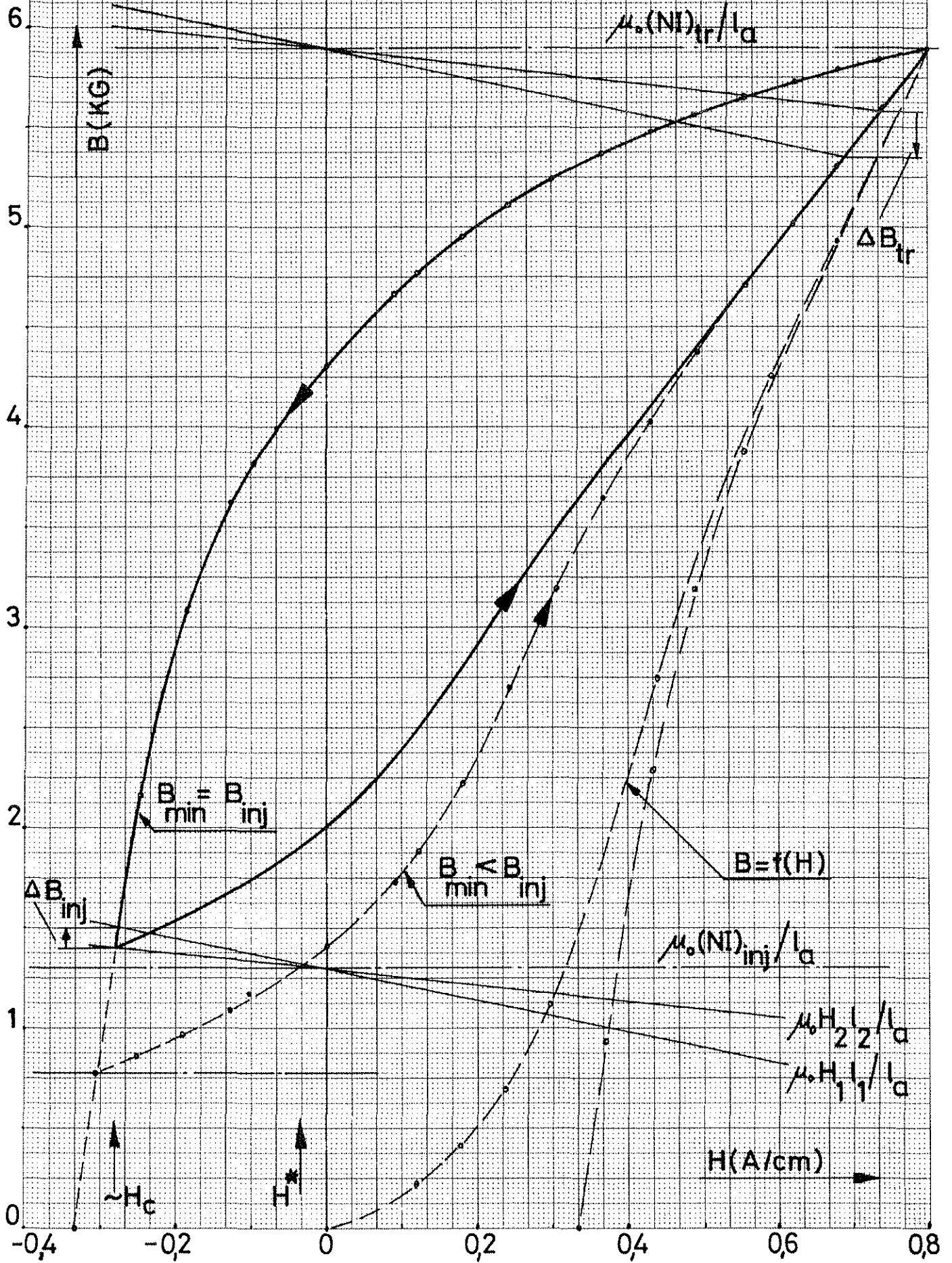
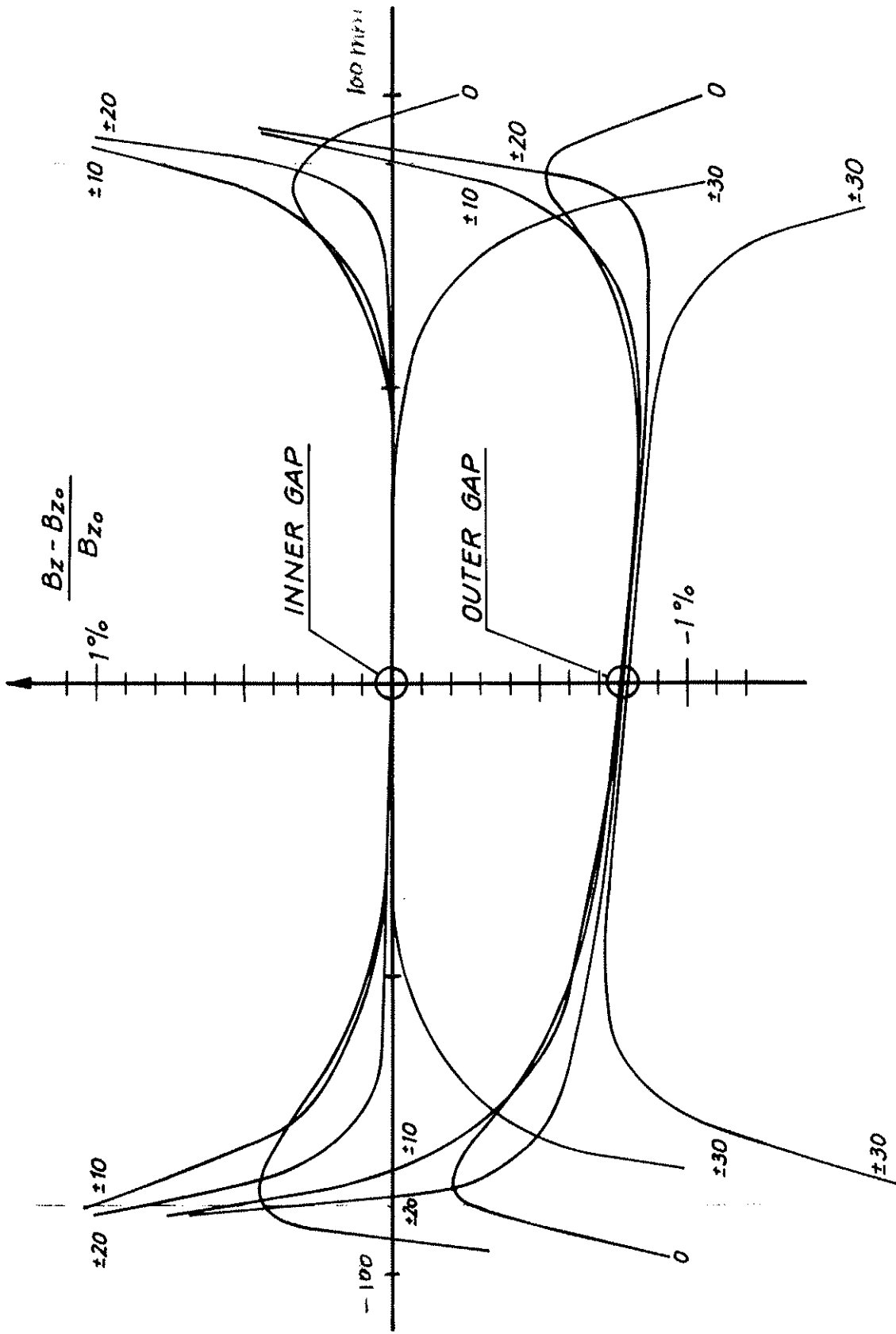


FIG.3 Magnetic Characteristics of Steel Supply

Hysteresis loop corresponding to Booster cycle  
(schematic) Fig 4.





**FIG. 5 BOOSTER BENDING MAGNET FIELD DISTRIBUTION**  
 **$B_{z0} = 5974$  Gs (SPECIFIED STEEL)**



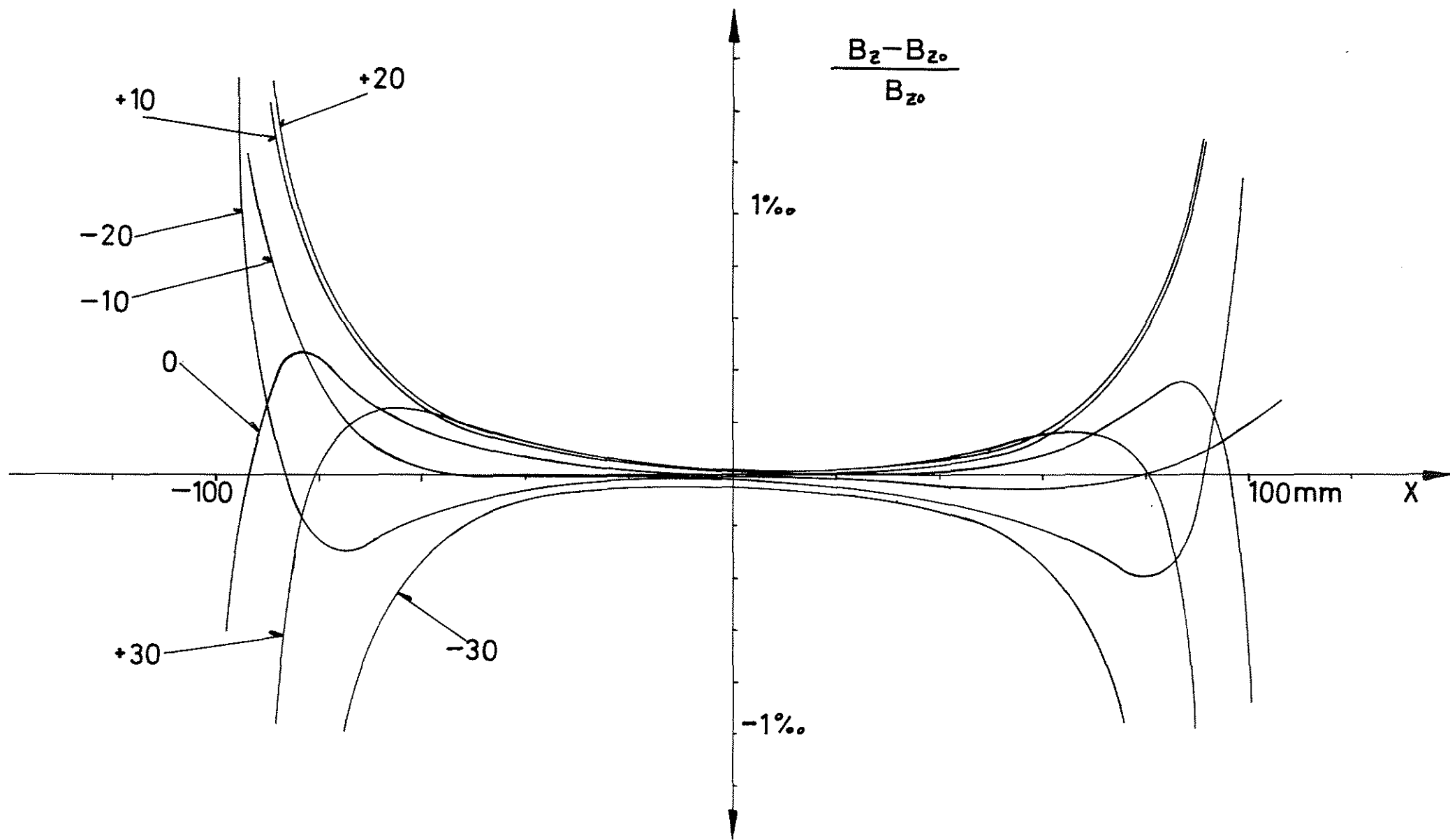
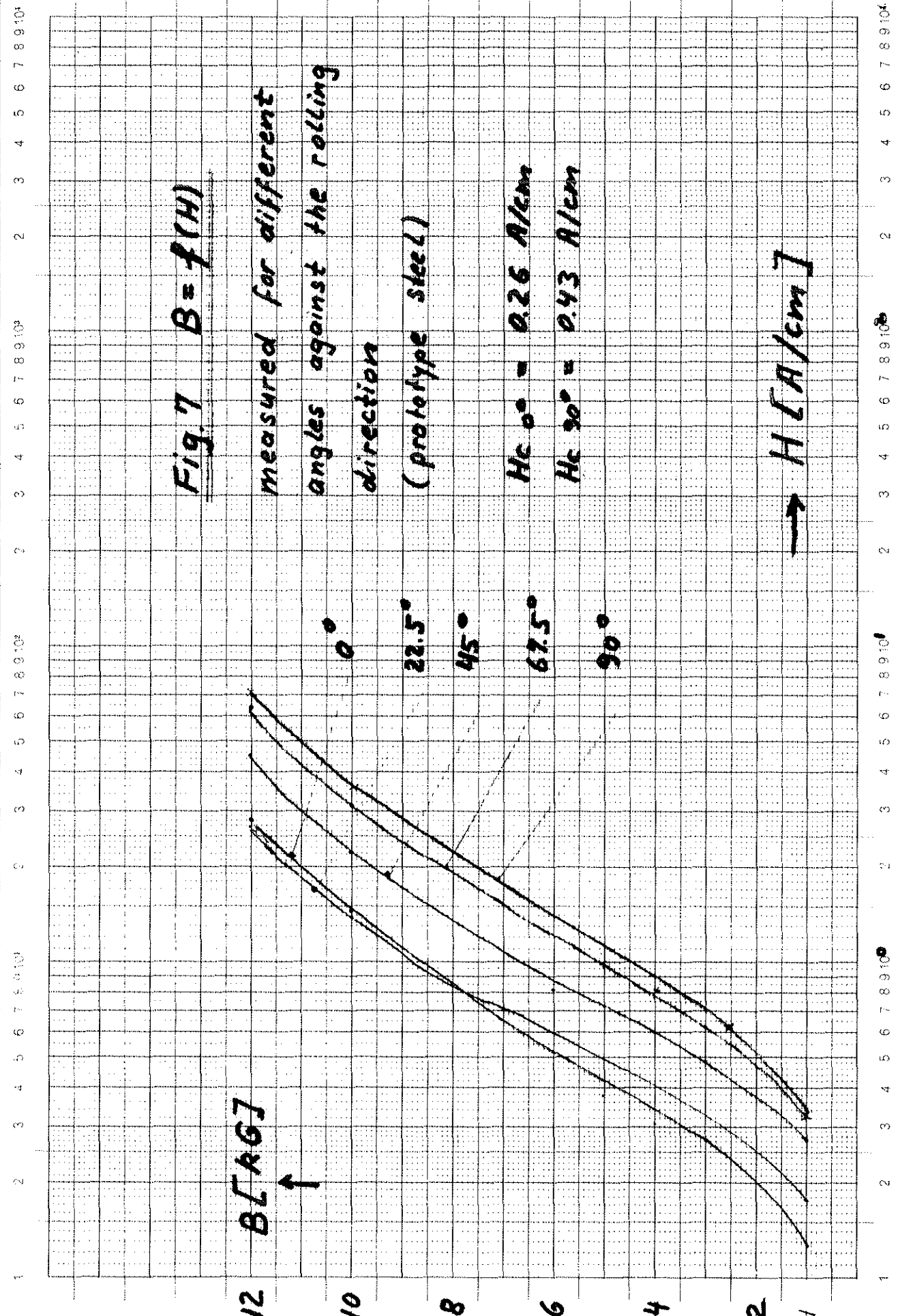
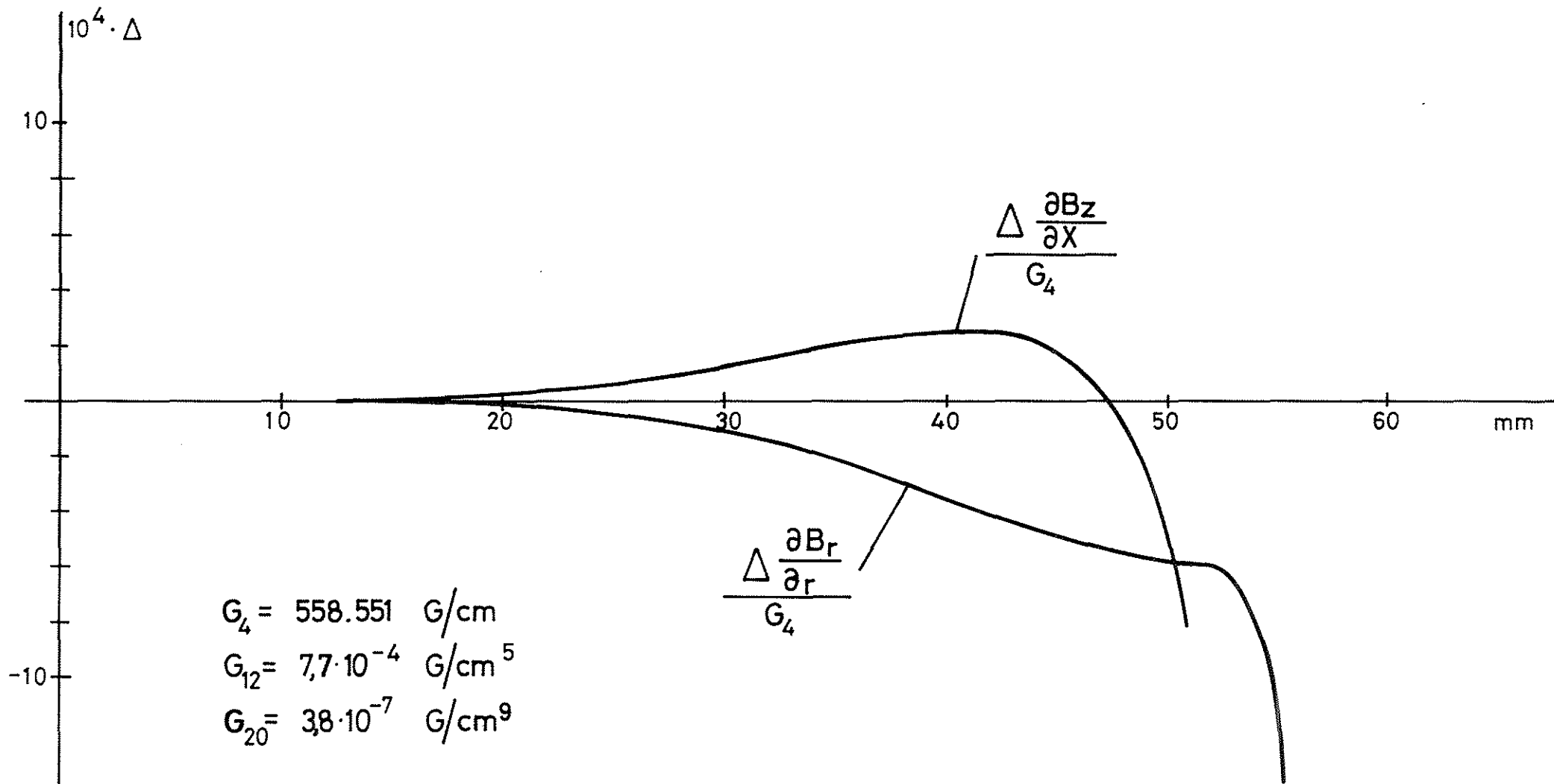


FIG.6 Booster B. M. field distribution inner gap, specified steel,  $B_{z_0} = 5974$  Gs.  
Coil displaced by  $\Delta z = 0,3$ mm





BOOSTER QUADRUPOLE (SYMMETRICAL)  
Gradient error

FIG. 8

FIG. 9

Flux distribution in the quadrupole for anisotropic distribution of magn. characteristics in the lamination  
 (from stainless steel plate model)

